Critical Point Fluctuations in Heavy-Ion Collisions within Molecular Dynamics with Expansion

Volodymyr A. Kuznietsov[1,3,*], *Volodymyr* Vovchenko[1], *Volker* Koch[2], and *Mark I.* Gorenstein[3]

[1]Physics Department, University of Houston, 3507 Cullen Blvd, Houston, TX 77204, USA

[2]Nuclear Science Division, Lawrence Berkeley National Laboratory, 1 Cyclotron Road, Berkeley, CA 94720, USA

[3]Department of the high-density Energy Physics, Bogolyubov Institute for Theoretical Physics, 03680 Kyiv, Ukraine

Abstract. We analyze particle number fluctuations near the critical endpoint of a first-order phase transition using molecular dynamics simulations of the Lennard-Jones fluid. Building on our previous study [V.A. Kuznietsov et al., Phys. Rev. C **105**, 044903 (2022)], we incorporate longitudinal collective flow. The scaled variance of particle number distributions in various coordinate and momentum space acceptances is computed through ensemble averaging, confirming previous time-averaging results. We find that significant collective flow is crucial for observing large fluctuations from the critical point in momentum space. These results are discussed in the context of heavy-ion collisions.

1 Introduction

Identifying the QCD critical point (CP) at finite baryon density remains a primary objective in beam energy scans of heavy-ion collisions [1]. Proton number fluctuations and their cumulants are critical for CP detection [2, 3], as non-monotonic behavior in cumulants is expected near the CP [4]. Recent measurements [5] observed excess variance below 20 GeV, exceeding predictions from baryon conservation and repulsive interactions [6]. Prior molecular dynamics (MD) simulations of the Lennard-Jones (LJ) fluid demonstrated strong CP signals in coordinate space, but they disappeared in momentum space due to a lack of particle correlations in the uniform LJ system [7, 8]. In this work, we extend our analysis to heavy-ion conditions. Using ensemble averaging over multiple events, in line with the ergodic hypothesis [9], and incorporating longitudinal flow (correlating momenta with coordinates), we assess whether large fluctuations remain detectable within experimentally relevant acceptances.

2 Simulation setup

2.1 Lennard-Jones Fluid

The LJ fluid consists of classical non-relativistic particles interacting via the potential:

$$V_{LJ}(r) = 4\varepsilon\left[\left(\frac{\sigma}{r}\right)^{12} - \left(\frac{\sigma}{r}\right)^{6}\right]. \tag{1}$$

---

*e-mail: vkuzniet@cougarnet.uh.edu

The first term represents short-range repulsion, while the second models intermediate-range attraction. Parameters σ and ε define the repulsive core size and attractive well depth, respectively, setting the system's length and energy scales.

Using dimensionless variables, we define the reduced temperature $\tilde{T} = T/(k_B \varepsilon)$, density $\tilde{n} = n\sigma^3$, and time $\tilde{t} = t\sqrt{\varepsilon/(m\sigma^2)}$. In these terms, most LJ fluid properties, including the phase diagram, become independent of σ and ε.

While the LJ equation of state is not exact, it has been extensively studied via molecular dynamics (MD). Its phase diagram includes a first-order liquid-gas transition with a critical point (CP) in the 3D-Ising universality class [10], located at $\tilde{T}_c = 1.321 \pm 0.007$ and $\tilde{n}_c = 0.316 \pm 0.005$ [11].

2.2 Molecular Dynamics

MD simulations integrate Newton's equations of motion using the Velocity-Verlet method for N particles with periodic boundary conditions [12]. In our previous work, we studied particle number fluctuations along the supercritical isotherm $\tilde{T} = 1.06\tilde{T}_c$ by simulating for extended periods and computing the moments of particle number distributions as time averages.

Here, we replicate the conditions of Ref. [8] using the same GPU-accelerated MD code [13]. The key difference is that we now calculate observables as ensemble averages by performing multiple simulations with random initial conditions at each density. This allows us to compare ensemble and time averaging, and to study equilibration dynamics. Our simulations use $N = 400$ particles, corresponding approximately to the number of baryons in central heavy-ion collisions when baryon-antibaryon pair production is negligible.

3 Incorporating longitudinal flow

In heavy-ion collisions, collective flow causes correlations between particle coordinates and momenta during the final stage of hydrodynamic evolution. To explore this, we incorporate longitudinal flow into our simulations to study fluctuations in rapidity acceptance, relevant to heavy-ion collisions. We focus on the longitudinal direction, integrating out transverse momenta. The longitudinal rapidity y for each particle is defined as the sum of collective and thermal components:

$$y = y^{\text{coll}} + y^{\text{th}}, \quad \text{where} \quad y^{\text{th}} = \sqrt{\frac{T_{\text{frz}}}{m_N \tilde{T}}} \, \tilde{v}_z^{\text{LJ}}. \tag{2}$$

In LJ fluid simulations, where there is no collective motion, the thermal rapidity component is $y^{\text{th}} \propto \tilde{v}_z^{\text{LJ}}$, with $\tilde{v}_z^{\text{LJ}}$ following a Maxwell-Boltzmann distribution with width $\sigma_{\tilde{v}_z^{\text{LJ}}} = \sqrt{\tilde{T}}$. In heavy-ion collisions, the thermal rapidity distribution width is $\sigma_y = \sqrt{T_{\text{frz}}/m_N}$, leading to the expression for y^{th}.

The collective rapidity component y^{coll} corresponds to space-time rapidity η_s in the Bjorken picture, where $y_{\text{coll}} = \eta_s$. The LJ longitudinal coordinate $\tilde{z}^{\text{LJ}}$ maps to η_s using:

$$y_{\text{cm}}^{\text{beam}}(\sqrt{s_{\text{NN}}}) = \ln\left[\frac{\sqrt{s_{\text{NN}}} + \sqrt{s_{\text{NN}} - 4m_N^2}}{2m_N}\right], \quad \text{thus} \quad y^{\text{coll}} = \frac{2y_{\text{cm}}^{\text{beam}}}{\tilde{L}} \tilde{z}^{\text{LJ}}. \tag{3}$$
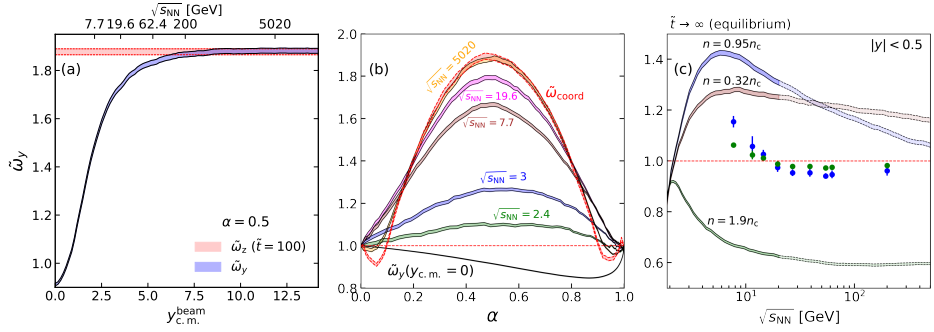
Figure 1. The corrected scaled variance with the effect of collective flow. Panels (a) and (b) stands for the density $n = 0.95n_c$ and temperature $T = 1.06T_c$ and panel (c) depicts $n = 0.32n_c, 0.95n_c$ and $1.9n_c$ for the same temperature. Panel (a) shows the flow at constant $\alpha = 0.5$ as a function of collision energy $\sqrt{s_{NN}}$. Panel (b) shows the same quantity for different α. Panel (c) depicts $\tilde{\omega}_y$ as a function of $\sqrt{s_{NN}}$ for fixed y_{cut}. The points correspond to the experimental data of the STAR Collaboration [5] for protons (green) and reconstructed baryons (blue).

We assume a flat particle density in space-time rapidity η_s, implying boost invariance up to the beam rapidity. Future work may explore non-uniform η_s distributions.

The described procedure is the simplest way to incorporate longitudinal flow, transforming a single fireball in a box into an expanding one. It follows the Bjorken picture and assumes no event-by-event fluctuations in longitudinal flow. For more precise applications, especially at lower RHIC beam energies, this model requires refinement. However, we use this simplified model to estimate the longitudinal flow effect under the most favorable conditions.

4 Results

4.1 Fluctuations at fixed α

We examine the fluctuations by the scaled variance defined as

$$\tilde{\omega}_y = \frac{1}{1-\alpha}\left[\frac{\langle N^2 \rangle - \langle N \rangle^2}{\langle N \rangle}\right], \tag{4}$$

with baryon conservation correction [14] at different energies for a fixed α, adjusting y_{cut} at each energy to satisfy $\alpha = \langle N_{acc}\rangle/N$ as depicted on Fig. 1 in panels (a) and (b). As y_{beam} increases, $\tilde{\omega}_y$ rises and eventually saturates at a value consistent with coordinate space fluctuations. This shows that strong collective flow maps coordinate space fluctuations onto momentum space. For $y_{beam} \to 0$, the results match box simulations where momentum space fluctuations are absent.

4.2 Fluctuations at fixed y_{cut}

In heavy-ion collisions, measurements are usually performed within a fixed rapidity interval near midrapidity, such as in STAR measurements of proton number cumulants. Fixing y_{cut} leads to a smaller α at higher energies due to the increased total rapidity coverage.

In Fig. 1(c) we observe that baryon number fluctuations in a fixed rapidity interval behave as expected for systems with a critical point. In the case of $n = 0.95n_c$, the fluctuations reflect the assumption that freeze-out near the CP occurs at a specific collision energy. However, the interplay between the finite lifetime and system size can suppress fluctuations in real systems.

5 Discussion and summary

In this article, we explore particle number fluctuations near the critical endpoint of a first-order phase transition using molecular dynamics simulations of the Lennard-Jones fluid. We found that collective flow is crucial for detecting large fluctuations in momentum space, similar to how those are observed in heavy-ion collisions. This study shows that the best signals for the CP can be observed in the 5–7 GeV collision energy range.

Future studies in the framework of molecular dynamics on higher statistics could include obtaining of the next two cumulants with and without the collective flow, testing different types of cumulants as a CP indicator, mixed phase studies, cross-check the results with Yukawa potential and utilizing of the AI for the phase diagram mapping.

6 Acknowledgments

References

[1] A. Bzdak, S. Esumi, V. Koch, J. Liao, M. Stephanov and N. Xu, Mapping the Phases of Quantum Chromodynamics with Beam Energy Scan, Physics Reports, **853** (2020)

[2] M. A. Stephanov, K. Rajagopal and E. Shuryak, Event-by-event fluctuations in heavy ion collisions and the QCD critical point, Phys. Rev. D **60** 114028 (1999)

[3] Y. Hatta and M. A. Stephanov, Proton number fluctuation as a signal of the QCD critical endpoint, Phys. Rev. Lett. **91** 102003 (2003)

[4] M. A. Stephanov, Non-Gaussian fluctuations near the QCD critical point, Phys. Rev. Lett. **102** 032301 (2009)

[5] M. Abdallah and al., Cumulants and correlation functions of net-proton, proton, and antiproton multiplicity distributions in Au+Au collisions at energies available at the BNL Relativistic Heavy Ion Collider, Phys. Rev. C **104** 024902 (2021)

[6] V. Vovchenko, QCD at finite temperature and density: Criticality, EPJ Web Conf. **296** 01017 (2024)

[7] V. A. Kuznietsov, O. Savchuk, R. V. Poberezhnyuk, V. Vovchenko, M. I. Gorenstein and H. Stöker, Molecular dynamics analysis of particle number fluctuations in the mixed phase of a first-order phase transition, Phys. Rev. C **107** 055206 (2023)

[8] V. A. Kuznietsov. O. Savchuk, M. I. Gorenstein, V. Koch and V. Vovchenko, Critical point particle number fluctuations from molecular dynamics, Phys. Rev. C **105** 044903 (2022)

[9] V. A. Kuznietsov, M. I. Gorenstein, V. Koch and V. Vovchenko, Coordinate versus momentum cuts and effects of collective flow on critical fluctuations, Phys. Rev. C **110** 015206 (2024)

[10] S. Stephan, J. Staubach and H. Hasse, Review and comparison of equations of state for the Lennard-Jones fluid, **523** 112772 (2020)

[11] S. Stephan, M. Thol, J. Vrabec and H. Hasse, Thermophysical Properties of the Lennard-Jones Fluid: Database and Data Assessment, Journal of Chemical Information and Modeling **59** 4248-4265 (2019)

[12] M. P. Allen and D. J. Tildesley, Computer Simulation of Liquids, Oxford University Press (2017)

[13] V. Vovchenko, Molecular dynamics simulation and visualization of the Lennard-Jones system utilizing CUDA-enabled GPUs (GitHub repository), https://github.com/vlvovch/lennard-jones-cuda

[14] V. Vovchenko, O. Savchuk, R. V. Poberezhnyuk, M. I. Gorenstein and V. Koch, Connecting fluctuation measurements in heavy-ion collisions with the grand-canonical susceptibilities, Phys. Lett. B **811** 135868 (2020)